

Peer review information: *Nature Communications* thanks the anonymous reviewers for their contribution to the peer review of this work.

Phase I clinical trial repurposing all-trans retinoic acid as a stromal targeting agent for pancreatic cancer .

Hemant M Kocher^{1,2,3,4*}, Bristi Basu⁵, Fieke EM Froeling^{6a}, Debashis Sarker⁷, Sarah Slater³, Dominic Carlin⁸, Nandita M deSouza⁸, Katja N De Paepe⁸, Michelle R Goulart¹, Christine Hughes¹, Ahmet Imrali⁴, Rhiannon Roberts⁴, Maria Pawula⁹, Richard Houghton⁹, Cheryl Lawrence², Yathushan Yogeswaran², Kelly Mousa², Carike Coetzee², Peter Sasieni^{10b}, Aaron Prendergast², David J Propper^{2,3,11}

Institutions (need full address):

141. Centre for Tumour Biology, Barts Cancer Institute- a CRUK Centre of Excellence, Queen Mary University London, London, EC1M 6BQ. UK.

162. Centre for Experimental Cancer Medicine, Barts Cancer Institute- a CRUK Centre of Excellence, Queen Mary University of London, London, EC1M 6BQ. UK.

183. Barts and the London HPB Centre, The Royal London Hospital, Barts Health NHS Trust, Whitechapel, London, E1 1FR. UK.

204. Barts Pancreas Tissue Bank, Barts Cancer Institute- a CRUK Centre of Excellence, Queen Mary University London, London, EC1M 6BQ. UK.

225. Department of Oncology, University of Cambridge and Cambridge University Hospitals NHS Foundation Trust - Addenbrooke's Hospital, Cambridge, CB2 0QQ. UK

246. Department of Surgery and Cancer, Imperial College London – Hammersmith Hospital, London, W12 0HS. UK

267. School of Cancer and Pharmaceutical Sciences, King's College London, Guy's Hospital Campus, London, SE1 9RT. UK

288. Division of Radiotherapy and Imaging, The Institute of Cancer Research, London, SW7 3RP.
29 UK.

309. PK/Bioanalytics Core Facility, Cancer Research UK Cambridge Institute, University of
31 Cambridge, Li Ka Shing Centre, Robinson Way, Cambridge, CB2 0RE. UK

3210. Cancer Prevention Trials Unit, Wolfson Institute of Preventive Medicine, Queen Mary
33 University of London, London, EC1M 6BQ. UK

3411. Centre for Cancer and Inflammation, Barts Cancer Institute- a CRUK Centre of Excellence,
35 Queen Mary University London, London, EC1M 6BQ. UK.

36

37 **Current addresses:**

38a. Cold Spring Harbor Laboratory, 1 Bungtown Road, Cold Spring Harbor, NY, 11724. USA

39b. School of Cancer & Pharmaceutical Sciences, and King's Clinical Trials Unit, King's College
40 London, London, SE1 9RT. UK

41

42 ***Corresponding author:**

43 Prof. Hemant. M. Kocher, MD, MS, FRCS

44 Professor of Liver and Pancreas Surgery

45 Centre for Tumour Biology, Barts Cancer Institute

46 Queen Mary University of London

47 London, EC1M 6BQ

48 Tel: +44 20 7882 3573 Fax +44 20 7882 3884

49 Email: h.kocher@qmul.ac.uk

50

51 [Abstract](#)

52 Pre-clinical models have shown that targeting pancreatic stellate cells with all-trans-retinoic-
53 acid (ATRA) reprograms pancreatic stroma to suppress pancreatic ductal adenocarcinoma
54 (PDAC) growth. Here, in a phase Ib, dose escalation and expansion, trial for patients with
55 advanced, unresectable PDAC (n=27), ATRA is re-purposed as a stromal-targeting agent in
56 combination with gemcitabine-nab-paclitaxel chemotherapy using a two-step adaptive
57 continual re-assessment method trial design. The maximum tolerated dose (MTD) and
58 recommended phase 2 dose (RP2D, primary outcome) is the FDA approved dose of
59 gemcitabine-nab-paclitaxel along-with ATRA (45 mg/m² orally, days 1-15 / cycle). Dose
60 limiting toxicity (DLT) is grade 4 thrombocytopenia (n=2). Secondary outcomes show no
61 detriment to ATRA pharmacokinetics. . Median overall survival for RP2D treated evaluable
62 population, is 11.7 months (95%CI 8.6-15.7m, n=15, locally advanced (2) and metastatic
63 (13)). Exploratory pharmacodynamics studies including changes in diffusion-weighted (DW)-
64 MRI measured apparent diffusion coefficient after one cycle, and, modulation of cycle-
65 specific serum pentraxin 3 levels over various cycles indicate stromal modulation. Baseline
66 stromal-specific retinoid transport protein (FABP5, CRABP2) expression may be predictive
67 of response. Re-purposing ATRA as a stromal-targeting agent with gemcitabine-nab-
68 paclitaxel is safe and tolerable. This combination will be evaluated in a phase II randomized
69 controlled trial for locally advanced PDAC. Clinical trial numbers: EudraCT: 2015-002662-23;
70 NCT03307148. Trial acronym: STARPAC.

71

72 Introduction

73 Advanced PDAC has a dismal prognosis with modestly effective treatment options.
74 Desmoplastic stroma and hypo-vascularity, distinctive features of PDAC, impede successful
75 delivery of chemotherapeutic drugs. Pancreatic stellate cells (PSC), critical components and
76 instigators of desmoplasia, mediate cancer cell pro-survival and pro-invasive capabilities
77 through multiple signalling cascades¹. This tumour-stroma cross-talk is unlikely to be
78 blocked effectively by merely targeting a single pathway. Targeting the multi-faceted tumour-
79 promoting cancer-stromal cell interactions (i.e., normalising the desmoplastic stroma) may,
80 however, enhance the effectiveness of conventional chemotherapy.

81

82 Patients with PDAC display fat-soluble vitamin deficiencies due to impaired biliary and
83 pancreatic secretions. Although vitamin K deficiency is manifested and treated clinically, the
84 lack of vitamin A², which is not recognised clinically, may perpetuate PSC activation. In a
85 healthy pancreas, PSC store a metabolite [retinoic acid (RA)] of vitamin A (retinol). When
86 activated, in cancer or inflammation, PSC lose RA stores and assume an activated
87 myofibroblast phenotype¹. Furthermore, RA also is a vital molecule regulating key signalling
88 pathways guiding embryonic pancreas development^{3,4}; signalling cascades that are hijacked
89 during pancreatic carcinogenesis.

90

91 Based on these observations, we demonstrated, using various PDAC models, that restoring
92 RA depots within PSC, using ATRA, limited the desmoplasia and suppressed cancer
93 growth^{1,5-7}. Furthermore, we established that activated PSC impede the migration of immune
94 cells, such as CD8⁺ T-cells, Natural Killer and B-cells, into the immediate PDAC
95 microenvironment; a process which was reversed by ATRA⁵. ATRA is an ideal agent to
96 dampen multiple, amplified, embryonic, context-specific signalling cascades activated in
97 PDAC^{7,8}. ATRA, but not 9-cis- or 13-cis-retinoic acid, reduces PSC proliferation by G1 cell-
98 cycle arrest with accumulation of lipid droplets, thus restoring their normal physiological role.
99 Specificity of retinoid (RAR) and rexinoid (RXR) receptor isoforms, distinctly used and

regulated by various RA, is vital in pancreatic embryogenesis and PSC biology⁹. Our data suggest a specific up-regulation of RAR β isoform by ATRA⁷. This is relevant, since 13-cisRA has previously been found to be ineffective, in combination with either gemcitabine¹⁰ or Interferon¹¹ in patients with PDAC.

Since only ATRA is relevant to PSC physiology and embryonic development of the pancreas, here we re-purpose ATRA as a stromal targeting agent, in combination with one of the widely used standard-of-care chemotherapy¹² in a phase Ib clinical trial. We demonstrate that ATRA is a stromal targeting by conducting pharmacokinetic and pharmacodynamic studies to discover specific biomarkers whilst determining recommended phase 2 dose (RP2D).

Results

Trial design and enrolment

We used an innovative two-step, adaptive, Bayesian continual reassessment method using five potential dose levels (DL) which appears to have advantages over standard 3+3 and titeCRM designs in accurately predicting RP2D, based on priors of toxicity data¹³ (Fig. 1, Supplementary Fig. 1, Supplementary Table 1). A total of 32 patients were screened to enrol 28 of whom 27 received any treatment from February 2016 to February 2018. Final data collection cut-off for clinical parameters was 1 April 2019.

Primary and secondary outcomes

We demonstrated that the FDA/EMA approved doses of gemcitabine (G, 1000mg/m² iv), nab-paclitaxel (nP, 125mg/m² iv), both on days 1, 8 and 15 of each 28-day cycle (PDAC¹²), can be combined safely with the recommended dose of ATRA (for acute promyelocytic leukaemia, APML¹⁴) at 45 mg/m² orally in two divided doses from days 1-15 of each cycle in patients with PDAC, resulting in an acceptable toxicity and side-effect profile (Dose Level 5 (DL5), Table 1, Fig. 1,2, Supplementary Tables 1-5). Thus, the primary outcome of Maximum tolerated dose (MTD) and recommended phase 2 dose (RP2D) was dose level 5. Two patients had dose limiting toxicities of grade 4 thrombocytopenia (one patient each at Dose Levels 3 and 5). Amongst secondary outcomes on safety and tolerability, neurotoxicity, characteristically seen with nab-paclitaxel treatment, appeared to be reduced by ATRA, in frequency and intensity, an aspect to be explored in larger randomised studies. This feature was previously reported in the context of lung cancer¹⁵, although with no underlying mechanistic explanation¹⁶.

Furthermore, patients treated at the MTD demonstrated encouraging evidence of response when assessed by best response of change in the target lesion sum of diameters compared to baseline (Fig. 2B). Median progression-free survival (PFS) was 6.4m (95%CI, 3.5m- not reached (NR)) and median overall survival (OS) was 10.9m (95%CI, 8.6m-NR)

(Supplementary Table 4) in the evaluable population (receiving at least two cycles of this combination or progressing within the first two cycles, n=15) analysis restricted to pre-specified follow-up for 12 months only for RP2D. Post-hoc analysis of these patients (n=15), of data beyond 12m, showed that the median OS of 11.7m (95%CI, 8.6-15.7m) for RP2D may be superior to the reported (8.5m, 95%CI: 7.9-9.5m) for metastatic PDAC in the phase III clinical trial with gemcitabine-nab-paclitaxel¹². Additionally, four of these patients (27%) went on to have second-line treatment (FOLFIRINOX, FOLFIRI, FOLFOX, 5FU+liposomal irinotecan (n=1 for each)), which was a lower proportion when compared to the pivotal phase III trial (38-42%)¹². Accepting that this is an early phase I trial, these are promising results.

ATRA pharmacokinetics

The addition of chemotherapy did not reduce plasma levels of ATRA (Fig. 3A, Supplementary Fig. 2-3, Supplementary Tables 6-7) when compared to historical data of single-agent ATRA at similar doses in patients without PDAC^{17,18}. The ATRA regimen at RP2D (at a dosing and schedule optimised for APL¹⁹), resulted in consistent plasma ATRA concentrations (AUC and Cmax) during successive cycles, strongly suggesting lack of CYP26 enzyme induction, a key factor limiting continued dosing with ATRA²⁰. Patient compliance with scheduling was excellent, with better median dose intensities of both cytotoxic agents than previously reported in the phase III trial for gemcitabine-nab-paclitaxel (Supplementary Table 5)¹².

Biochemical response and Vitamin A levels

CA19-9 biochemical responses are a reliable predictor of long-term survival in PDAC^{12,21}. Whilst most patients (14/19 at RP2D) showed significant early and sustained CA19-9 responses, we identified five patients who had a poor CA19-9 response (Fig. 3B-C, Supplementary Fig. 4). Plasma vitamin A levels for most patients were maintained throughout all cycles, implying no induction of CYP26 enzyme-mediated clearance. The five patients who had poor CA19-9 responses exhibited either a lower starting, or a decline in

levels of plasma vitamin A during course of therapy, which upon linear regression analysis demonstrated a downward trend as opposed to steady levels for patients with a biochemical response (Fig. 3D-F, Supplementary Fig. 5). This implies that plasma vitamin A levels could potentially be a surrogate pharmacodynamic marker as a composite readout of absorption and metabolism of retinol which is upstream of, and therefore distinct from, ATRA absorption and metabolism. An added benefit is the convenience of a routine assay in hospital laboratories. Optimal biological dose (OBD) using vitamin A levels greater than or equal to $1\mu\text{mol/L}$ and less than or equal to $2.5\mu\text{mol/L}$, on an exploratory basis²², was achieved in 67-82% of patients in each of the cycles (cycle 1 (72%, n=18), cycle 2 (82%, n=11), cycle 3 (82%, n=11), cycle 4 (67%, n=9), cycle 5 (75%, n=8) and cycle 6 (67%, n=9) for DL5 patients whom vitamin A levels were available and excluding any patients who had dose modifications from the point of modification onwards (Supplementary Table 8). These data led to ATRA dosing, as described in DL5, to be taken forward as RP2D.

Exploratory biomarkers: DW-MRI

Several potential biomarkers have emerged from this phase I study which might be employed in future studies. Since repeated biopsies of primary tumours are not practical and may be ethically demanding, we used an imaging biomarker as a surrogate for stromal activity. The dense cellular stroma reduces tissue water content. Diffusion-weighted (DW)-MRI allows derivation of an apparent diffusion coefficient (ADC), which reflects extra- and intra-cellular water mobility²³, and can be a robust imaging biomarker for response assessment in human tumours, if appropriately protocolled for cross-platform analysis (Supplementary Tables 9-10, Supplementary Fig. 6)²⁴. Hence we evaluated ATRA's stromal effect using the true diffusion (D) component of ADC. True diffusion (D) values demonstrated a consistent increase as early as one month after treatment, indicating stromal modulation, where there is no change in tumour volume, indicating stromal modulation²⁵, as observed in our preclinical models⁷ (Fig. 4A-D).

Exploratory biomarkers: tissue assays

The baseline biopsies assessed for retinoic acid transport molecules in cancer and stromal cell compartments, demonstrated a differential distribution of fatty acid binding protein 5 (FABP5) and cellular retinoic acid binding protein 2 (CRABP2)²⁶, using a well-validated method to distinguish stromal and epithelial compartments²⁷, such that patients with increased stromal expression of FABP5 were more likely to achieve disease control (Fig. 4E-G; Supplementary Fig. 7,8, Supplementary Table 11). Thus the stromal expression of FABP5 can be explored as a potential predictive biomarker.

Exploratory biomarkers: serum assays

Since we demonstrated previously that pentraxin 3 gene (*PTX3*) is upregulated in activated PSC, and can be used as a potential diagnostic biomarker for pancreatic cancer²⁸, we explored whether serum PTX3 could act as a stromal-response biomarker. An upregulation of serum PTX3 within five hours of administering ATRA on days 1 and 8 of the first cycle, an effect lost by day 15, indicated that continuous administration of ATRA may not have a sustained stromal effect (Fig. 4H, Supplementary Fig. 9). Upregulation of serum PTX3 was not demonstrable by cycle 6 of the treatment when the median serum PTX3 was at the upper limit of normal, as seen in healthy subjects, perhaps indicating the maximum duration of ATRA therapy should be six months (Fig. 4I). Serum PTX3 will be explored further in the context of a planned randomised controlled trial where comparisons can be made with non-ATRA treated patients.

Discussion

The promising results of this phase I study support stromal normalisation as a valid approach in chemotherapeutically intractable cancers such as PDAC. We demonstrate that re-purposing ATRA as a stromal targeting agent, with gemcitabine-nab-paclitaxel, is safe and tolerable with an exciting potential to enhance delivered chemotherapy dose intensity, and mitigating some of the expected adverse events, such as neurotoxicity, with evidence of putative pharmacodynamic readouts. These features are in contrast to recently publicized negative results of HALO 109-031 trial targeting stroma using pegvorhyaluronidase alfa (PEGPH20), an agent which potentially increases adverse events²⁹.

This translation of pre-clinical work to a clinical application, based on clinical observations and repurposing existing drugs, should be tested in other diseases where stromal normalisation could impact clinical outcome. Based on the encouraging response and survival data seen here, the efficacy of this regimen will be evaluated in a phase II randomised clinical trial in locally advanced PDAC (NCT04241276), incorporating pharmacodynamic biomarkers for ATRA and stromal targeting, and genomic readouts of tumoural³⁰ and stromal³¹ heterogeneity, which may play role in differential response.

238 Methods

239 Trial design and patient population

240 STARPAC was an open-label, multicenter, phase Ib study of ATRA administered with
241 gemcitabine and nab-paclitaxel in patients with locally advanced or metastatic pancreatic
242 cancer, who had not received prior systemic therapy for their disease. Additional eligibility
243 criteria included World Health Organisation (WHO) performance status 0 or 1, life
244 expectancy ≥ 12 weeks and adequate hematologic and end-organ function within 14 days
245 prior to the first study treatment. Major exclusion criteria were known brain metastases, pre-
246 existing sensory neuropathy ($>$ grade 1) and serious medical risk factors involving any major
247 organ systems, or serious psychiatric disorders, which could compromise the patient's safety
248 or the study data integrity.

249

250 There were two parts to this study. In Part 1, a dose-escalation strategy using the two-step
251 adaptive Bayesian continual reassessment method (CRM)¹³ was used to determine the MTD
252 and the recommended dose to be taken forward in Part 2, a dose expansion phase, to
253 explore the OBD. OBD initially defined by vitamin A levels between 1.5 and 2.5 μM (both
254 inclusive) at each cycle was post-trial closure modified to levels of 1 and 2.5 μM (both
255 inclusive) in line with National Institute of Health's Office of Dietary Supplements'
256 recommended levels²². OBD was estimated at 80% of patients achieving serum vitamin A
257 levels.

258

259 All patients provided written informed consent. Ethical approval for STARPAC clinical trial;
260 South Central - Berkshire Research Ethics Committee (REC); 15/SC/0548 dated 13 October
261 2015 (Supplementary Note 1: Trial Protocol). STARPAC trial was prospectively registered
262 with EudraCT (2015-002662-23) on 11 June 2015 and clinical trial.gov (NCT03307148) on
263 11 October 2017. Trial opened to recruitment on 20 January 2016. Three substantial
264 amendments were made to clinical trial protocol, and details are available on EudraCT.
265 Permission for post-hoc analysis for data beyond 12 months of study was obtained from

South Central - Berkshire REC on 24 July 2019. All clinical data were collected on an in-house built electronic Case Report Form (eCRF) designed using ORACLE v11.2.0. The study was sponsored by Barts Health NHS Trust. The Centre for Experimental Cancer Medicine (CECM), Barts Cancer Institute, Queen Mary University of London had overall responsibility for trial management. The Trial Management Group (TMG) was responsible for day-to-day running of the trial. Safety data was reviewed regularly by the Safety Review Committee (SRC).

Statistical analysis

It was expected that a maximum of 24 evaluable patients would be enrolled into Part 1 of the study based on CRM¹³. For Part 1, the primary objective was to determine the MTD of the combination of gemcitabine-nab-paclitaxel and ATRA, measured by the occurrence of DLTs during the first 28 days of treatment that were attributed as possibly, probably or definitely related to the study treatment. For Part 2, a sample size of 10 was considered reasonable to provide indicative data on OBD.

Secondary endpoints included analyses of PK parameters, response rates, progression-free survival (PFS), overall survival (OS), and safety. For all time-to-event analyses performed, patients who did not have an event were right censored: - PFS censored on the last date the patient was known to be progression-free; OS censored at the date of last contact within 12 months of enrolment into trial. Post-hoc OS analysis was carried out for data beyond 12 months after REC approval to include data as there were exceptional survivors. Survival endpoints were shown graphically with Kaplan-Meier plots.

All efficacy analyses were performed on the evaluable population which included all patients receiving at least two cycles of the combination or progressing within the first two cycles, regardless of whether they were later found to be ineligible or a protocol violator. Safety analyses included all patients who received at least one dose of study treatment. The worst

grade of each adverse event (AE) for each patient during study treatment was reported. Cumulative dose intensity over the first 6 cycles was calculated as the actual amount of study drug received over the first 6 cycles divided by the expected amount of study drug received over the first 6 cycles. The expected amount of study drug was calculated based on the dose and schedule specified in the study protocol.

Sample size calculations were performed using the software package PASS version 12.0. All clinical efficacy endpoints were analyzed using STATA version 13.1. Laboratory data were analyzed using PRISM (GraphPad Inc) version 8. Statistical tests are described as used.

Sample storage and traceability

All samples had a valid chain of custody throughout procurement, temporary storage at site, shipping, and permanent storage at the Barts Pancreas Tissue Bank (BPTB, REC Ref: 13/SC/0592, HTA License number: 12199) and were given to laboratory staff via a traceable database, in a blinded, anonymized manner.

Pharmacokinetic assays

ATRA, 9-cis-RA and 13-cis-RA were purchased from Sigma Aldrich (Poole, UK), and ATRA-d5 from Toronto Research Chemicals (North York, Ontario, Canada). Liquid chromatography mobile phase solvents (water, acetonitrile and formic acid), were Optima grade, purchased from Fisher Scientific (Loughborough, UK). An analytical method, using LC-MS/MS, was established for the measurement of all-trans retinoic acid concentrations in plasma. The method was subject to EMEA validation procedures³². Validation of this method included precision and accuracy, selectivity, specificity, matrix effects (including hemolytic and hyperlipidaemic plasma), effect of co-medications, carryover, re-injectability, stability in whole blood, stability of stock and working solutions and stability assessments in plasma (24h room temperature, 4 freeze/thaw cycles, and long term frozen storage at both -20°C and -80°C).

All analyses were done using an AB Sciex 6500 mass spectrometer (Warrington, UK) equipped with a Nexera 2 LC-system (Shimadzu, MA, USA). Internal standard ATRA-d5 was added to 10 μ L of patient plasma sample. The plasma proteins were precipitated using acetonitrile, followed by vortexing and centrifugation. Supernatants (150 μ L) were transferred to clean wells in a 96-well plate, followed by the addition of 50 μ L water and vortex mixing. Calibration standards (calibration range 50 to 5000 ng/mL) and QC samples (100, 300, 800 and 4000 ng/mL) were prepared by the addition of ATRA to blank human plasma, and then processed in the same manner as patient samples (Supplementary Fig. 2, Supplementary Table 7).

The extracts were analyzed by reversed phase chromatography (Acquity BEH C18 UPLC column, Waters Corp., MA, USA), using gradient elution with acetonitrile and 0.1% formic acid, at a flow rate 0.4 ml/min, total run duration 10min. This was coupled to the MS/MS detector, operating in positive ion atmospheric pressure chemical ionization mode. The MS/MS transitions for ATRA and internal standard ATRA-d5 were m/z 301 > 205 and m/z 306 > 206, respectively. The declustering potential, collision energy and collision exit potential were; 40V, 20V and 12V, respectively, both for ATRA and ATRA-d5. A minimum of six quality control samples were included in each LC-MS/MS run. ATRA calibration standards were prepared in the calibration range 50 to 5000 ng/mL using pooled human plasma. Standards and samples were assayed in the same manner using the internal standard ATRA-d5. Quality control samples at 100, 300, 800 and 4000 ng/ml were used to determine accuracy and precision (Supplementary Fig. 2, Supplementary Table 7).

Pharmacokinetic data were calculated using Prism software (GraphPad) and validated against PCModfit software (<http://pcmodfit.co.uk/nca.html>) with substitution of all 'below limits of quantification' levels of ATRA at zero (range could be zero to 62.5ng/ml).

DW-MRI

MRI was performed at two institutions on multivendor platforms (Supplementary Table 9). Longitudinal studies on the same patient were undertaken on the same scanner. The protocols were developed to maximize signal-to-noise ratio and minimize ghosting and distortion using a well-validated test object³³.

Scans were done at baseline and at day 22-28 after treatment. Test object measurements for quality-assurance of quantitative metrics were undertaken regularly to ensure quality control. The coefficient of variation (CV) for Apparent Diffusion Coefficient (ADC) across multiple time-points was 0.4% and 1.4% (Philips and GE respectively). ADC CV between the two sites was 3.9%. MRI examinations consisted of DW-MRI of the abdomen and pelvis as per the protocols below, followed by T₁-weighted and T₂-weighted imaging in matched positions.

Diffusion-weighted MRI Analysis

On the pre- and post-treatment scans, regions-of-interest (ROI) were drawn around the tumor on the high b-value ($b = 800 \text{ s/mm}^2$) diffusion-weighted images by a board-certified radiologist in OsiriX version 9.0. ROIs were then copied onto the corresponding ADC maps which were generated on a voxel-by-voxel basis from a mono-exponential fit to the data as described by: $S(b) = S(0) \exp(-b \cdot \text{ADC})$.²⁴

Tissue CRABP2, FABP5

H&E quality control of remaining tissue from diagnostic material by a board-certified pathologist for histological / cytological confirmation demonstrate that there was either inadequate tissue (n=7) or only cancer cells without stroma (n=5), to carry further analysis. Hence formalin-fixed paraffin-embedded (FFPE) sections from 15 patients were dewaxed and rehydrated, antigen retrieved (0.1M citrate buffer, pH 6, microwave, 20m), blocked (1h,

RT, 2% bovine serum albumin, 0.02% fish skin gelatin, 10% FBS, 5% goat serum) before use of primary antibodies at 4°C overnight, followed by appropriate fluorescent-labelled secondary antibodies ²⁷. The nuclei were then counterstained with DAPI. Organotypic sections, from as previous experiments⁷, were used for positive and negative staining controls (Supplementary Table 11). Controls were uniformly negative with appropriate isotype-specific immunoglobulin at matching dilutions.

Immunofluorescent images were taken using the Zeiss Confocal LSM510 microscope at 20x magnification, and images were visualized using Zeiss Zen 2.3 software. The green channel represented either α -SMA or CK; the red channel represented FABP5 or CRABP2. The intensity of fluorescence in the green/red channel for respective molecules was given a semi-quantitative value, ranging from negative “-” through to strongly positive “+++”. There were 4 categories of fluorescence intensity: -, +, ++, +++. The threshold gain and offset was set according to the intensity of the green/red channel in the organotypic cultures, and ensured minimal inter-day variability (Supplementary Fig. 7,8).

Plasma PTX3

PTX3 levels were quantified with a sandwich ELISA using in-house validated protocol based on a monoclonal antibody MNB4 (Enzo Life Sciences ALX-804-464-C100) ³⁴. Plasma PTX3 concentrations were quantified using the sandwich ELISA as follows: 96 well-ELISA plates were coated with MNB4 anti- human PTX3 antibody (100 ng/well) diluted in coating buffer (15mM carbonate buffer, pH 9.6, overnight, 4°C), washed, blocked (5% dry milk in washing buffer, 2h, room temperature), washed and incubated with either 50 μ l of diluted plasma (1:3 dilution in PBS without Ca^{++} Mg^{++} and 2% BSA) or 50 μ l recombinant human PTX3 standards (0.31-20 ng/ml), all in duplicates for 2h at 37°C. After two washes, 50 ng/ml of biotinylated PTX3 (Enzo Life Sciences, cat. ALX-210-365B) antibody was added in each well for 1h at RT, washes and color realized by 100 μ l/well streptavidin-horseradish peroxidase (Amersham, cat. RPN4401V) diluted 1:4,000 for 1h at RT. After further washes 100 μ l of

chromogen substrate (ThermoFisher cat. 34028B) was added and plates read after 15min at 450 nm in a plate-reader. Polynomial regression graphs were constructed for standard curves. Plasma samples of each patient time-point were thawed only once and assayed, maintaining a chain of custody, in duplicate. ELISA was conducted in a blinded manner, and inter-day variability standard patient samples were used with CV 0.17 (Supplementary Fig. 9). Patient variables were unblinded after submission of readouts.

Data availability

The data supporting this Article are available within the Article, Supplementary Information or available from the authors upon request.

419 References

- 420 1. Froeling, F.E., *et al.* Retinoic acid-induced pancreatic stellate cell quiescence reduces
421 paracrine Wnt- β -catenin signaling to slow tumor progression. *Gastroenterology* **141**, 1486-
422 1497, 1497.e1481-1414 (2011).
- 423 2. Huang, X., *et al.* Association between vitamin A, retinol and carotenoid intake and pancreatic
424 cancer risk: Evidence from epidemiologic studies. *Sci Rep.* **6:38936.**, 10.1038/srep38936.
425 (2016).
- 426 3. Stafford, D. & Prince, V.E. Retinoic acid signaling is required for a critical early step in
427 zebrafish pancreatic development. *Curr Biol* **12**, 1215-1220 (2002).
- 428 4. Huang, W., *et al.* Retinoic acid plays an evolutionarily conserved and biphasic role in
429 pancreas development. *Dev Biol.* **394**, 83-93. doi: 10.1016/j.ydbio.2014.1007.1021. Epub
430 2014 Aug 1013. (2014).
- 431 5. Ene-Obong, A., *et al.* Activated pancreatic stellate cells sequester CD8+ T cells to reduce their
432 infiltration of the juxtatumoral compartment of pancreatic ductal adenocarcinoma.
433 *Gastroenterology* **145**, 1121-1132 (2013).
- 434 6. Di Maggio, F., *et al.* Pancreatic stellate cells regulate blood vessel density in the stroma of
435 pancreatic ductal adenocarcinoma. *Pancreatology* (2016).
- 436 7. Carapuca, E.F., *et al.* Anti-stromal treatment together with chemotherapy targets multiple
437 signalling pathways in pancreatic adenocarcinoma. *J Pathol* **239**, 286-296 (2016).
- 438 8. Froeling, F.E. & Kocher, H.M. Homeostatic restoration of desmoplastic stroma rather than its
439 ablation slows pancreatic cancer progression. *Gastroenterology* **148**, 849-850 (2015).
- 440 9. Micallef, S.J., *et al.* Retinoic acid induces Pdx1-positive endoderm in differentiating mouse
441 embryonic stem cells. *Diabetes* **54**, 301-305 (2005).
- 442 10. Michael, A., Hill, M., Maraveyas, A., Dalglish, A. & Lofts, F. 13-cis-Retinoic acid in
443 combination with gemcitabine in the treatment of locally advanced and metastatic
444 pancreatic cancer--report of a pilot phase II study. *Clin Oncol (R Coll Radiol)* **19**, 150-153
445 (2007).
- 446 11. Brembeck, F.H., *et al.* A phase II pilot trial of 13-cis retinoic acid and interferon-alpha in
447 patients with advanced pancreatic carcinoma. *Cancer* **83**, 2317-2323 (1998).
- 448 12. Von Hoff, D.D., *et al.* Increased survival in pancreatic cancer with nab-paclitaxel plus
449 gemcitabine. *N Engl J Med* **369**, 1691-1703 (2013).
- 450 13. North, B., Kocher, H.M. & Sasieni, P. A new pragmatic design for dose escalation in phase 1
451 clinical trials using an adaptive continual reassessment method. *BMC Cancer.* **19**, 632. doi:
452 610.1186/s12885-12019-15801-12883. (2019).
- 453 14. Burnett, A.K., *et al.* Inclusion of chemotherapy in addition to anthracycline in the treatment
454 of acute promyelocytic leukaemia does not improve outcomes: results of the MRC AML15
455 trial. *Leukemia* **27**, 843-851 (2013).
- 456 15. Arrieta, O., *et al.* Randomized phase II trial of All-trans-retinoic acid with chemotherapy
457 based on paclitaxel and cisplatin as first-line treatment in patients with advanced non-small-
458 cell lung cancer. *J Clin Oncol* **28**, 3463-3471 (2010).
- 459 16. Albers, J.W., Chaudhry, V., Cavaletti, G. & Donehower, R.C. Interventions for preventing
460 neuropathy caused by cisplatin and related compounds. *Cochrane Database Syst Rev.*,
461 CD005228. doi: 005210.001002/14651858.CD14005228.pub14651854. (2014).
- 462 17. Jing, J., *et al.* Physiologically Based Pharmacokinetic Model of All-trans-Retinoic Acid with
463 Application to Cancer Populations and Drug Interactions. *J Pharmacol Exp Ther.* **361**, 246-
464 258. doi: 210.1124/jpet.1117.240523. Epub 242017 Mar 240528. (2017).
- 465 18. Zang, Y., Lee, J.J. & Yuan, Y. Adaptive designs for identifying optimal biological dose for
466 molecularly targeted agents. *Clinical trials (London, England)* **11**, 319-327 (2014).
- 467 19. Kanamaru, A., *et al.* All-trans retinoic acid for the treatment of newly diagnosed acute
468 promyelocytic leukemia. Japan Adult Leukemia Study Group. *Blood.* **85**, 1202-1206. (1995).

20. Stevison, F., Jing, J., Tripathy, S. & Isoherranen, N. Role of Retinoic Acid-Metabolizing Cytochrome P450s, CYP26, in Inflammation and Cancer. *Adv Pharmacol* **74**:373-412., 10.1016/bs.apha.2015.1004.1006. Epub 2015 May 1027. (2015).
21. Chiorean, E.G., *et al.* CA19-9 decrease at 8 weeks as a predictor of overall survival in a randomized phase III trial (MPACT) of weekly nab-paclitaxel plus gemcitabine versus gemcitabine alone in patients with metastatic pancreatic cancer. *Ann Oncol*. **27**, 654-660. doi: 610.1093/annonc/mdw1006. Epub 2016 Jan 1022. (2016).
22. Office of Dietary Supplements, N. Vitamin A, Fact sheet for health professionals. Vol. 2020 Vitamin A (Office of Dietary Supplements, National Institute of Health, <https://ods.od.nih.gov/factsheets/VitaminA-HealthProfessional/>, 2020).
23. Matsumoto, Y., *et al.* In vitro experimental study of the relationship between the apparent diffusion coefficient and changes in cellularity and cell morphology. *Oncol Rep*. **22**, 641-648. doi: 610.3892/or_00000484. (2009).
24. deSouza, N.M., *et al.* Implementing diffusion-weighted MRI for body imaging in prospective multicentre trials: current considerations and future perspectives. *Eur Radiol*. **28**, 1118-1131. doi: 1110.1007/s00330-00017-04972-z. Epub 02017 Sep 00327. (2018).
25. Wegner, C.S., Gaustad, J.V., Andersen, L.M., Simonsen, T.G. & Rofstad, E.K. Diffusion-weighted and dynamic contrast-enhanced MRI of pancreatic adenocarcinoma xenografts: associations with tumor differentiation and collagen content. *J Transl Med*. **14**, 161. doi: 110.1186/s12967-12016-10920-y. (2016).
26. Gupta, S., *et al.* Molecular determinants of retinoic acid sensitivity in pancreatic cancer. *Clin Cancer Res* **18**, 280-289 (2012).
27. Hughes, C.S., ChinAleong, J.A. & Kocher, H.M. CRABP2 and FABP5 expression levels in diseased and normal pancreas. *Ann Diagn Pathol* **47**, 151557 (2020).
28. Watt, J., *et al.* Role of PTX3 in pancreatic cancer. *Lancet* **383**, 57 (2014).
29. Tempero, M.A., *et al.* HALO 109-301: A randomized, double-blind, placebo-controlled, phase 3 study of pegvorhyaluronidase alfa (PEGPH20) + nab-paclitaxel/gemcitabine (AG) in patients (pts) with previously untreated hyaluronan (HA)-high metastatic pancreatic ductal adenocarcinoma (mPDA). *Journal of Clinical Oncology* **38**, 638-638 (2020).
30. Bailey, P., *et al.* Genomic analyses identify molecular subtypes of pancreatic cancer. *Nature*. **531**, 47-52. doi: 10.1038/nature16965. Epub 12016 Feb 16924. (2016).
31. Neuzillet, C., *et al.* Inter- and intra-tumoural heterogeneity in cancer-associated fibroblasts of human pancreatic ductal adenocarcinoma. *J Pathol*. **248**, 51-65. doi: 10.1002/path.5224. Epub 2019 Feb 1022. (2019).
32. EMEA. Guideline on bioanalytical method validation. (ed. CHMP) (EMA, Brussels, 2011).
33. Winfield, J.M., *et al.* A framework for optimization of diffusion-weighted MRI protocols for large field-of-view abdominal-pelvic imaging in multicenter studies. *Med Phys*. **43**, 95. doi: 10.1118/1.111.4937789. (2016).
34. Latini, R., *et al.* Prognostic significance of the long pentraxin PTX3 in acute myocardial infarction. *Circulation* **110**, 2349-2354 (2004).

Acknowledgements

This paper is dedicated to the patients who participated in the clinical trial and Dr Irene Kaimi, statistician who was involved in early statistical analysis but tragically died before it was completed. We thank the trial coordinators at the Barts Centre for Experimental Cancer Medicine for help in the setting up and conduct of the STARPAC trial as well as NIHR Clinical Research Facility and ECMC at each site (Imperial, Cambridge, Kings, Barts). We thank Bernard North for designing the statistical framework for the trial. This work was supported by grants from Medical Research Council (MR/M015610/1, HMK) and Celgene Sarl (AX-CL-Panc-PI-003922, HMK) who funded the study and supplied drugs (Celgene; nab-paclitaxel). Pancreatic Cancer Research Fund Tissue Bank grant supports BPTB. The funders had no role in design or analysis of this study nor preparation of this manuscript.

Contributions

PS, HMK designed the trial. Patient recruitment and trial monitoring was done by BB, FEMF, DS, SS, DP, CC, KM, CL HMK. MRI data was analyzed and summarized by DC, NMD, KNDP, HMK. Serum and tissue biomarker data was analyzed and summarized by MRG, CH, AI, RR, HMK. Pharmacokinetic data was analyzed and summarized by MP, RH, HMK. Statistical analysis was performed by YY, AP, HMK. Data was interpreted by DJP, AP, CC, HMK. First draft was written by HMK and all authors approved and commented on various drafts. HMK acts a guarantor.

Competing interests

HMK received research grant for conducting this trial (Celgene: institutional) and educational grant support for attending or organizing conferences (Celgene, Baxalta, Mylan, Medtronic, Oncosil: institutional) which are unrelated to this work. SS has consultancy with Eisai UK which have no direct relation to this work. BB has consulting role (Eisai Europe Limited, Roche, GenMab, Baxter Innovations, Celgene, Biocompatibles Ltd, Nordic Pharma SAS: all

538 payments to institution), is on speaker's bureau (Eisai Europe Limited) received research
539 funding (Celgene: investigator initiated trial), and has educational grant support for attending
540 conferences (Bayer, Celgene), all of which have no direct relation to this work. DS is on
541 advisory boards for Eisai, Novartis, Ipsen and Surface Oncology; speaker honoraria from
542 Astra Zeneca, Eisai, MSD and Bayer; travel sponsorship from Eisai, Ipsen and MiNA
543 Therapeutics, all of which have no direct relation to this work. The remaining authors declare
544 no conflict of interest.

545

546 Figure Legends

547 Figure 1. CONSORT diagram for STARPAC clinical trial.

548 Number of patients at all Dose Levels (DL) in dose-escalation, part 1 (using the STARPAC
549 adaptive trial design¹³) for maximum tolerated dose (MTD) estimation, showing Dose limiting
550 toxicity (DLT) and dose expansion (part 2) of the trial for optimal biological dose (OBD)
551 estimation leading to recommended phase 2 dose (RP2D).

552

553 Figure 2. Primary and secondary endpoints for STARPAC clinical trial.

554 a: Swimmer's plot with color code for different dose levels (DL) and duration (months) on X-
555 axis along with type of disease: locally advanced (LA) and metastatic (M), those who
556 experienced DLT (*) and disease status (Death (D), progressive disease (PD)) censored at
557 the pre-specified 12 months of starting on the trial.

558 b: Waterfall plot of best percentage change of sum of diameters in target lesion from
559 baseline in RP2D treated patients based on an evaluable population. A positive change
560 denotes an increase in the target lesion sum of diameters over time and, likewise, a negative
561 change denotes a decrease in the target lesion sum of diameters over time. Reference lines
562 added for response (-30% change in target lesion sum of diameters) and progression (20%
563 change in target lesion sum of diameters). RECIST responses are marked with asterisk (*).
564 There was progression for 6.7% (95% CI: 0.2-31.9%) and response in 46.7% (95% CI: 21.3-
565 73.4%) of patients.

566 c: Post-hoc (including data from beyond 12 months) estimated median overall survival in 15
567 patients receiving RP2D on evaluable population basis. Number of events =13. Kaplan-
568 Meier plot.

569

570 Figure 3: ATRA pharmacokinetics, biochemical CA19-9 response and vitamin A levels.

571 a: Serum ATRA levels for the first three cycles are summarized as mean (SEM) for the first
572 five hours after co-administration of ATRA at 45mg/m² with chemotherapy drugs.

b: Absolute CA19-9 levels on logarithmic Y-axis for patients on Dose Level 5 at start of each cycle. Summary statistics represented by box (median \pm interquartile range) and whisker (range: LQR-(1.5xIQR) and UQR+(1.5xIQR)). One-sided Skilling-Mack test, statistic 39.21, $p < 0.001$.

c: Normalized CA19-9 levels for each patient on Dose Level 5 with baseline being 100%. There were 14 biochemical responders (black) compared to 5 non-responders (unique colors). Responders are defined as those who show $>30\%$ reduction of CA19-9 from baseline with a sustained response (no greater than 20% rise from previous reading at any time).

d: Vitamin A on Dose Level 5 at start of each cycle. Summary statistics represented by box (median \pm interquartile range) and whisker (range: LQR-(1.5xIQR) and UQR+(1.5xIQR)). One-sided Skilling-Mack test, statistic 5.95, $p = 0.31$.

e: Individual values for vitamin A for patients with biochemical non-responders (CA19-9) highlighted in corresponding colors as in Panel c.

f: Linear regression trend lines comparing biochemical responders (solid line) to non-responders (dashed line) demonstrate that a drop in serum vitamin A levels may indicate non-responders. $N=X$ R: X is the number of responders at the stated cycle.

$N=X$ NR: X is the number of non-responders at the stated cycle.

Figure 4: Biomarkers for STARPAC clinical trial

a: MRI sequences as indicated with primary pancreatic tumor (red arrow) and liver metastasis (white arrow) in T2-weighted images for localization, both lesions demonstrating change in the apparent diffusion coefficient (ADC) within these tumors, after just one month of treatment, indicative of an increased mobile water content due to reduction in dense cellularity with a rim of peripheral restricted tissue represents residual tumor.

Summary statistics of changes in tumor volume (b), ADC values (c), and D values (d) between pre-treatment (baseline) and post-first-cycle (day 21-28) of treatment. Summary

data as mean \pm SEM. Data points represent values from individual patients. Two-tailed Wilcoxon matched-pairs sign-rank test.

e: Representative images of co-immuno-fluorescent images of pancreatic cancer biopsies prior to commencement of treatment, to assess prevalence of Cellular Retinoic Acid Binding Protein 2 (CRABP2) and Fatty Acid Binding Protein 5 (FABP5), as indicated with co-staining with either cytokeratin (CK) or alpha-smooth muscle actin (α SMA) respectively, to demonstrate a 3+ stain for both CRABP2 and FABP5 in cancer cells and cancer associated fibroblasts (CAF). Scale bar: 100 μ m.

f,g: These quantifications (range 0 to 3+) were then assessed for all evaluable biopsies (n=15) from single representative image using appropriate tissue controls and categorized according to disease control / progressive disease. Chi-square test. dF = 3

h: Measurement of serum PTX3 by ELISA (GCLP standards, CV 0.17) in patients before (Base) and five hours after (Post) taking ATRA in the first cycle (C1) on days 1, 8 and 15

i: Measurement of serum PTX3 five hours after taking ATRA on the first day of each cycle (1-6). Each point represents an individual patient.

h,i: Box (median \pm interquartile range) and whisker (full range). Individual measurements per patient represented as a dot derived from mean of two readings. Two-tailed Wilcoxon matched pairs signed rank test.

Table 1. Adverse events for STARPAC clinical trial. Distribution of AE. AE \geq grade 3 and DLTs in all patients and those receiving DL5 (RP2D) according to SOC term, whether attributable or not to treatment. *Indicates counts of each instance e.g. if one patient has the same term three times this is counted as 3 instances. N = Number of patients in the Safety Set population for the specified group of patients.

Figure 1

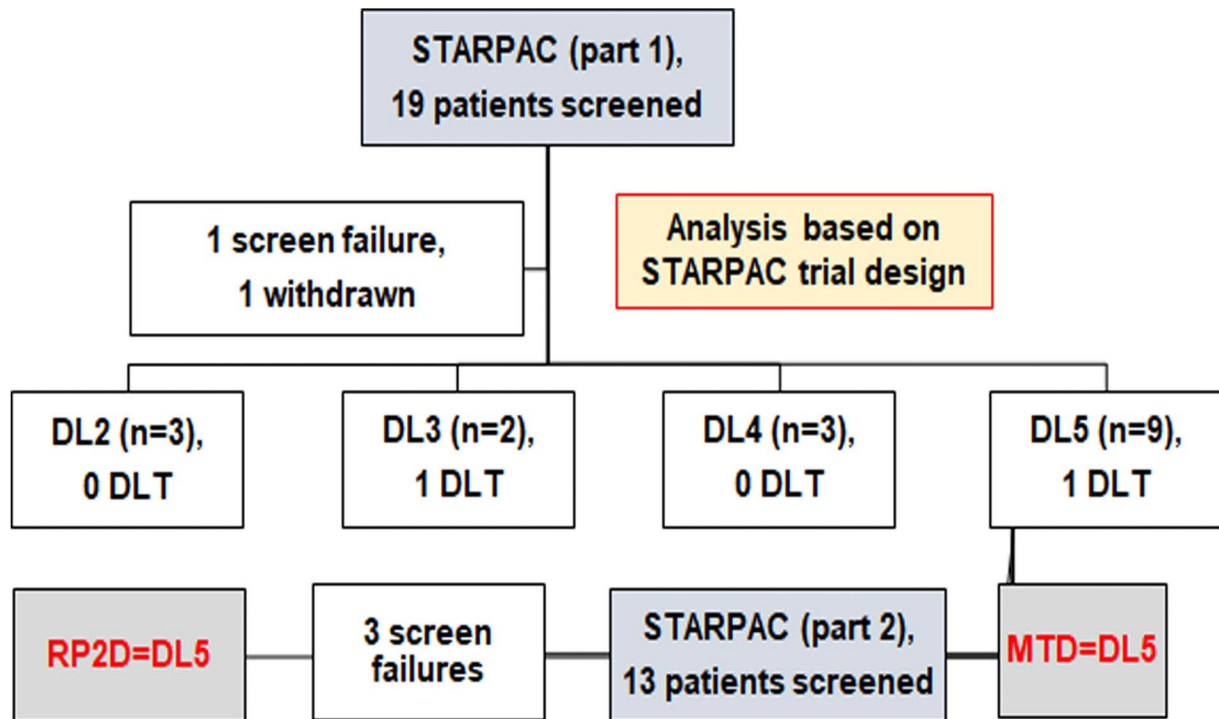


Figure 1. CONSORT diagram for STARPAC clinical trial. Number of patients at all Dose Levels (DL) in dose-escalation, part 1 (using the STARPAC adaptive trial design¹³) for maximum tolerated dose (MTD) estimation, showing Dose limiting toxicity (DLT) and dose expansion (part 2) of the trial for optimal biological dose (OBD) estimation leading to recommended phase 2 dose (RP2D).

Figure 2

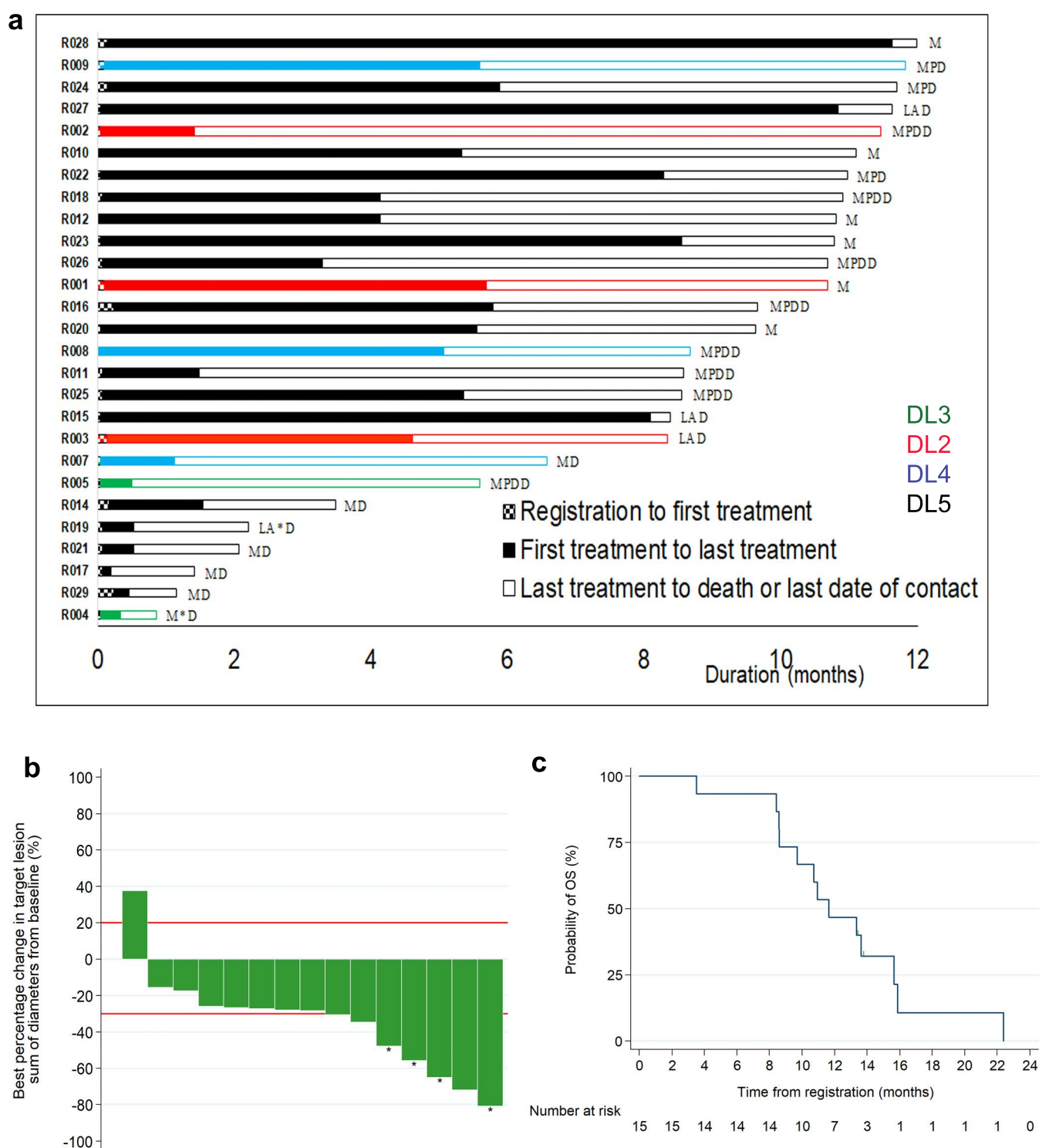


Figure 2. Primary and secondary endpoints for STARPAC clinical trial.

a: Swimmer's plot with color code for different dose levels (DL) and duration (months) on X-axis along with type of disease: locally advanced (LA) and metastatic (M), those who experienced DLT (*) and disease status (Death (D), progressive disease (PD)) censored at the pre-specified 12 months of starting on the trial.

b: Waterfall plot of best percentage change of sum of diameters in target lesion from baseline in RP2D treated patients based on an evaluable population. A positive change denotes an increase in the target lesion sum of diameters over time and, likewise, a negative change denotes a decrease in the target lesion sum of diameters over time. Reference lines added for response (-30% change in target lesion sum of diameters) and progression (20% change in target lesion sum of diameters). RECIST responses are marked with asterisk (*). There was progression for 6.7% (95% CI: 0.2-31.9%) and response in 46.7% (95% CI: 21.3-73.4%) of patients.

c: Post-hoc (including data from beyond 12 months) estimated median overall survival in 15 patients receiving RP2D on evaluable population basis. Number of events =13. Kaplan-Meier plot.

Figure 2

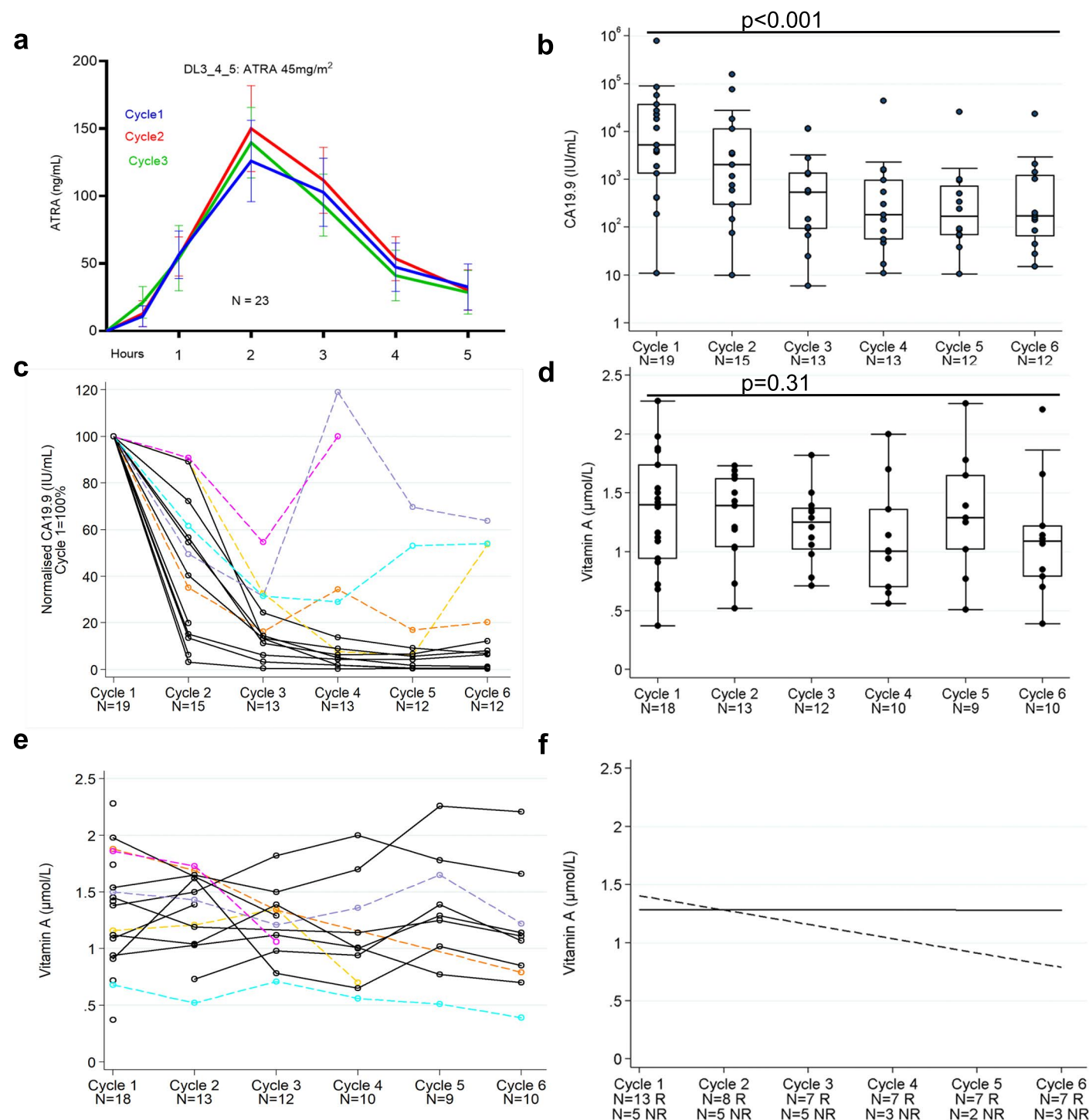


Figure 3: ATRA pharmacokinetics, biochemical CA19-9 response and vitamin A levels.

a: Serum ATRA levels for the first three cycles are summarized as mean (SEM) for the first five hours after co-administration of ATRA at 45mg/m² with chemotherapy drugs.

b: Absolute CA19-9 levels on logarithmic Y-axis for patients on Dose Level 5 at start of each cycle. Summary statistics represented by box (median ± interquartile range) and whisker (range: LQR-(1.5xIQR) and UQR+(1.5xIQR)). One-sided Skilling-Mack test, statistic 39.21, p < 0.001.

c: Normalized CA19-9 levels for each patient on Dose Level 5 with baseline being 100%. There were 14 biochemical responders (black) compared to 5 non-responders (unique colors). Responders are defined as those who show >30% reduction of CA19-9 from baseline with a sustained response (no greater than 20% rise from previous reading at any time).

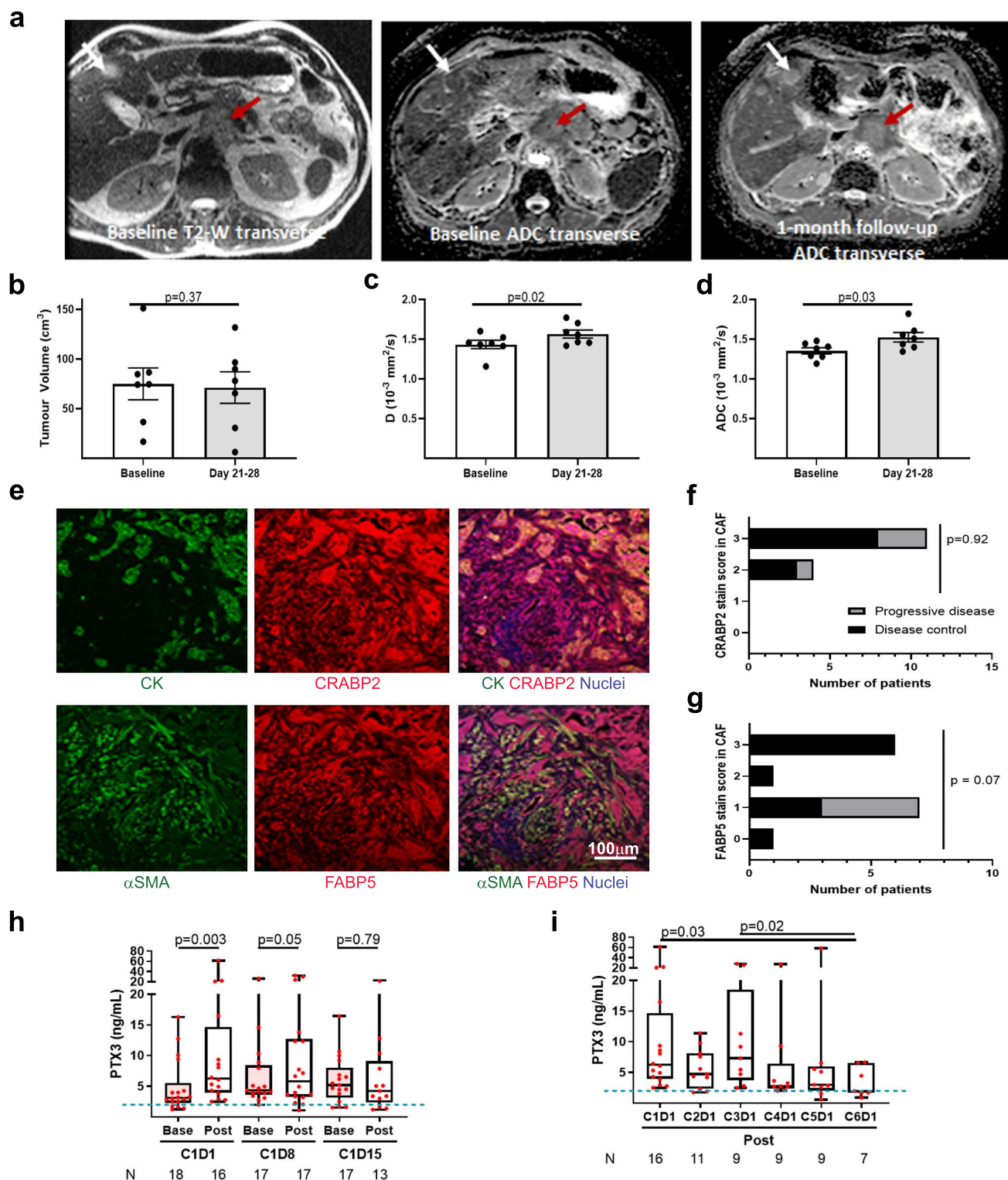
d: Vitamin A on Dose Level 5 at start of each cycle. Summary statistics represented by box (median ± interquartile range) and whisker (range: LQR-(1.5xIQR) and UQR+(1.5xIQR)). One-sided Skilling-Mack test, statistic 5.95, p = 0.31.

e: Individual values for vitamin A for patients with biochemical non-responders (CA19-9) highlighted in corresponding colors as in Panel c.

f: Linear regression trend lines comparing biochemical responders (solid line) to non-responders (dashed line) demonstrate that a drop in serum vitamin A levels may indicate non-responders.

N=X R: X is the number of responders at the stated cycle.

N=X NR: X is the number of non-responders at the stated cycle.

Figure 2**Figure 4: Biomarkers for STARPAC clinical trial**

a: MRI sequences as indicated with primary pancreatic tumor (red arrow) and liver metastasis (white arrow) in T2-weighted images for localization, both lesions demonstrating change in the apparent diffusion coefficient (ADC) within these tumors, after just one month of treatment, indicative of an increased mobile water content due to reduction in dense cellularity with a rim of peripheral restricted tissue represents residual tumor. Summary statistics of changes in tumor volume (**b**), ADC values (**c**), and D values (**d**) between pre-treatment (baseline) and post-first-cycle (day 21-28) of treatment. Summary data as mean \pm SEM. Data points represent values from individual patients. Two-tailed Wilcoxon matched-pairs sign-rank test.

e: Representative images of co-immuno-fluorescent images of pancreatic cancer biopsies prior to commencement of treatment, to assess prevalence of Cellular Retinoic Acid Binding Protein 2 (CRABP2) and Fatty Acid Binding Protein 5 (FABP5), as indicated with co-staining with either cytokeratin (CK) or alpha-smooth muscle actin (αSMA) respectively, to demonstrate a 3+ stain for both CRABP2 and FABP5 in cancer cells and cancer associated fibroblasts (CAF). Scale bar: 100 μm .

f,g: These quantifications (range 0 to 3+) were then assessed for all evaluable biopsies ($n=15$) from single representative image using appropriate tissue controls and categorized according to disease control / progressive disease. Chi-square test. $\text{dF} = 3$.

h: Measurement of serum PTX3 by ELISA (GCLP standards, CV 0.17) in patients before (Base) and five hours after (Post) taking ATRA in the first cycle (C1) on days 1, 8 and 15

i: Measurement of serum PTX3 five hours after taking ATRA on the first day of each cycle (1-6). Each point represents an individual patient. **h,i:** Box (median \pm interquartile range) and whisker (full range). Individual measurements per patient represented as a dot derived from mean of two readings. Two-tailed Wilcoxon matched pairs signed rank test.

Table 1. Adverse events for STARPAC clinical trial. Distribution of AE. AE \geq grade 3 and DLTs in all patients and those receiving DL5 (RP2D) according to SOC term, whether attributable or not to treatment. *Indicates counts of each instance e.g. if one patient has the same term three times this is counted as 3 instances. N = Number of patients in the Safety Set population for the specified group of patients.

Adverse events (AE) summary		
	DL5 Patients	All Patients
Total patients (N)	19	27
AEs reported, n	470	638
Patients with at least one AE, n	19	27
AEs per patient*, median (range)	23 (8 – 71)	23 (8 – 71)
\geq Grade 3 AEs* reported, n	33	55
Patients with at least one \geq Grade 3 AE, n	11	17
\geq Grade 3 AEs per patient*, median (range)	3 (1 – 5)	3 (1 – 9)